Published OnlineFirst July 20, 2010; DOI: 10.1158/1541-7786.MCR-10-0174

Molecular Cancer Research

p53-Dependent Induction of Prostate Cancer Cell Senescence by the PIM1 Protein Kinase

Marina Zemskova[1], Michael B. Lilly[6], Ying-Wei Lin[2], Jin H. Song[3], and Andrew S. Kraft[4,5]

Abstract

The PIM family of serine threonine protein kinases plays an important role in regulating both the growth and transformation of malignant cells. However, in a cell line–dependent manner, overexpression of PIM1 can inhibit cell and tumor growth. In 22Rv1 human prostate cells, but not in Du145 or RWPE-2, PIM1 overexpression was associated with marked increases in cellular senescence, as shown by changes in the levels of β-galactosidase (SA-β-Gal), p21, interleukin (IL)-6 and IL-8 mRNA and protein. During early cell passages, PIM1 induced cellular polyploidy. As the passage number increased, markers of DNA damage, including the level of γH2AX and CHK2 phosphorylation, were seen. Coincident with these DNA damage markers, the level of p53 protein and genes transcriptionally activated by p53, such as p21, TP53INP1, and DDIT4, increased. In these 22Rv1 cells, the induction of p53 protein was associated not only with senescence but also with a significant level of apoptosis. The importance of the p53 pathway to PIM1-driven cellular senescence was further shown by the observation that expression of dominant-negative p53 or shRNA targeting p21 blocked the PIM1-induced changes in the DNA damage response and increases in SA-β-Gal activity. Likewise, in a subcutaneous tumor model, PIM1-induced senescence was rescued when the p53-p21 pathways are inactivated. Based on these results, PIM1 will have its most profound effects on tumorigenesis in situations where the senescence response is inactivated. *Mol Cancer Res; 8(8); 1126–41. ©2010 AACR.*

Introduction

The PIM family of serine/threonine protein kinases has been implicated in the initiation or progression of multiple cancer types. The PIMs were initially cloned as proviral integration sites in Moloney murine leukemia virus–induced murine T-cell lymphomagenesis (1-3). In transgenic mouse models, the PIM family of protein kinases function as weak oncogenes stimulating T-cell lymphomas (1, 4) and can complement the activity of both c-MYC and AKT to enhance tumorigenesis (5-8). The induction of lymphomas in PIM-containing mice is markedly enhanced by treatment of these animals with chemical carcinogens (9) or γ-irradiation (10). The PIM protein kinases are overexpressed in many human cancers, including prostate cancer (11, 12), lymphoma (13, 14), leukemia (15), head and neck squamous cell carcinomas (16, 17), and pancreatic and colon cancers (18, 19). In human prostate, expression of PIM1 is low in benign prostatic hypertrophy, moderate in high grant intraepithelial neoplasia, and increased in frank cancer (11, 20). Both high Gleason grade and progression to aggressive metastatic prostate cancer has been associated with increased PIM levels (12, 21). Overexpression of PIM1 in human prostate cancer cells markedly increases their growth as tumors in animals (22).

Recent experiments have shown in normal fibroblasts that the overexpression of PIM1 can induce senescence rather than enhance growth (23). Oncogene-induced senescence (OIS) is well known and caused by multiple genes (24-27), including mutant RAS, RAF, and ERB-2 (for review, see refs. 28-30). Like other inducers of senescence, OIS is associated with a flattened cellular morphology; cell cycle arrest; stimulation of secretion of multiple cytokines, including interleukin (IL)-6 and IL-8; and activation of signaling networks driven by marked changes in the levels of specific transcription factors, for example, CEBP/β (31-33). Although the mechanism of OIS is complex, it seems to involve DNA replicative stress leading to the production of double-strand breaks and the recruitment of the serine-threonine kinase ataxia-telangiectasia mutated (ATM; refs. 34, 35). ATM enhances the activity of p53 directly and, through the phosphorylation of the CHK2 protein kinase, modifies the phosphorylation of the p53 protein (36, 37). The induction of OIS is associated with downstream activation of the p53 and pRb (38, 39) pathways

Authors' Affiliations: Departments of [1]Cell and Molecular Pharmacology, [2]Pediatrics, and [3]Biochemistry and Molecular Biology; [4]Hollings Cancer Center; and [5]Department of Medicine, The Medical University of South Carolina, Charleston, South Carolina; and [6]Chao Family Comprehensive Cancer Center, University of California, Irvine, California

Note: Supplementary data for this article are available at Molecular Cancer Research Online (http://mcr.aacrjournals.org/).

Corresponding Author: Andrew S. Kraft, Hollings Cancer Center, 86 Jonathan Lucas Street, Charleston, SC 29425. Phone: 843-792-8284; Fax: 843-792-9456. E-mail: Kraft@musc.edu

doi: 10.1158/1541-7786.MCR-10-0174

Published OnlineFirst July 20, 2010; DOI: 10.1158/1541-7786.MCR-10-0174

with increases in inhibitors of cyclin-dependent protein kinases, including $p16^{INK4a}$ and p21 (40-43), although OIS seems to proceed in p16 knockout mice (44). Activation of both c-MYC and RAS had been associated with the induction of a DNA damage response followed by OIS (45, 46). The induction of senescence as a result of the DNA damage response seems to depend on the extent of DNA damage, with minor changes being repaired (47). In precancerous lesions in animals and humans, OIS is a part of a tumorigenesis barrier imposed by DNA damage checkpoints (34). Because oncogenes are well known to induce cell death through the activation of the caspase cascade followed by apoptosis, there seems to be a critical balance between senescence and apoptosis, mediated in part by proteins that block cell death (i.e., BCL-2) and transcription factors (i.e., BRN-3a) that cooperate with p53 to induce growth inhibition rather than apoptosis (48).

Based on our observation that PIM1 overexpression in the human prostate cancer cell line 22Rv1, but not Du145, inhibits the growth of these cells, we have evaluated the ability of PIM1 overexpression to induce senescence and apoptosis in these human prostate cancer cells and studied the role of p53 and p21 in this process.

Materials and Methods

Reagents and plasmids

The following mouse monoclonal antibodies were used in these studies: anti-PIM1 and anti-human IL-6 (Santa Cruz Biotechnology), anti-human $p21^{CIP1/WAF1}$ (Transduction Laboratories, BD Biosciences), anti-cyclin B1 (Pharmigen, BD Biosciences), anti–γ-tubulin, and anti–glyceraldehyde-3-phosphate dehydrogenase (GAPDH)–peroxidase conjugated (Sigma). Additionally, rabbit monoclonal anti–Ki-67 and rabbit polyclonal anti-γH2AX antibodies were purchased from Abcam. Rabbit polyclonal antibodies used in these experiments include anti-p27 (Santa Cruz Biotechnology) and anti–dimethyl-histone H3 (Lys9; Millipore). Antibodies to p53 and phospho-CHK2 (Thr68) were purchased from Cell Signaling Technology, Inc. Fluorescein isothiocyanate–conjugated anti-mouse and Cy3-conjugated anti-rabbit antibodies were from Sigma. Doxycycline was purchased from Sigma and prepared as a stock solution at 2 mg/mL in PBS.

A p53-green fluorescent protein (p53-GFP) plasmid (plasmid 11770) was purchased from Addgene, and a retroviral vector encoding the dominant-negative variant of p53 (pBabe/p53DN) was kindly provided by Dr. Carola Neumann (Medical University of South Carolina, Charleston, SC). Lentiviral pTRIPz vectors encoding Tet-inducible control shRNA (RHS4743) and p21 shRNA (V2THS_202469) were purchased from Open Biosystems (Thermo Fisher Scientific, Inc.).

Retroviral vectors encoding PIM1 or a kinase-dead variant of PIM1 (KD PIM1) were designed as described previously (49). To generate inducible PIM1 expression constructs, the coding region for *PIM1* gene was inserted into the *Age*I-*Mlu*I sites of the pTRIPz/shRNA lentiviral vector (Open Biosystems). This procedure resulted to substitution of the RFP-shRNA cassette downstream of the Tet/ON promoter with the PIM1 cDNA. The pTRIPz vector with excision of RFP-shRNA cassette and without insertion of PIM1 was used as a vector control (pTRIPz). All of these constructs were verified by sequence analysis.

Cell culture, viruses, and generation of stable cell lines

Human prostate 22Rv1, Du145, RWPE-1, RWPE-2, and Cos7 cells were obtained from the American Type Culture Collection. 22Rv1 and DU145 cells were grown in RPMI 1640, and Cos7 cells were grown in Dulbecco's modified Eagle's medium (Thermo Fisher Scientific) supplemented with 10% fetal calf serum. RWPE-1 and RWPE-2 cells were maintained in keratinocyte medium supplemented with 5 ng/mL human recombinant epidermal growth factor and 0.05 mg/mL bovine pituitary extract (Invitrogen). Murine embryonic fibroblasts triple knockout for PIM1, PIM2, and PIM3 kinases (TKO MEF) were derived from 14.5-day-old embryos and were genotyped as described (50). The tissue culture medium was supplemented with 100 units/mL penicillin and 100 μg/mL streptomycin (Gibco).

The production of infectious retroviruses encoding PIM1, KD PIM1, dominant-negative p53 (DN p53), and vector control (pLNCX) was carried out as previously described (49). 293FT cells and the Trans-Lentiviral packaging system (Open Biosystems) were used to produce infectious lentiviruses according to the manufacturer's protocol.

To generate 22Rv1, Du145, RWPE-1, and RWPE-2 stable pools that constitutively express PIM1, cells were plated 16 to 18 hours before transduction at 1×10^5 cells/60-cm plates and then infected with 5×10^4 retroviral particles in the presence of 8 μg/mL Polybrene. After 6 hours of incubation, the virus-containing medium was replaced with fresh medium. On the next day, 400 μg/mL G418 was added to select the stably infected cell population. After 10 days of selection, stable cell pools were established, and the expression of PIM1 transgenes was verified by Western blot analysis.

For inducible PIM1 expression assays, 22Rv1, Cos7, or TKO MEF cells were infected with lentiviruses encoding vector control (pTRIPz) or PIM1 (pTRIPz/PIM1) using ViraDuctin Lentivirus Transduction Kit (Cell Biolabs, Inc.). Cells were selected with 5 μg/mL puromycin for 12 days. Individual clones were isolated, and cells were incubated in the absence or presence of doxycycline and subjected to Western blotting to analyze PIM1 expression.

Additional pools of 22Rv1 cells that overexpressed DN p53 were established through retroviral transduction. Stable cell lines derived from two individual clones expressing inducible PIM1 were infected with retroviruses encoding vector control (pLNCX) or DN p53 (pBabe/DN p53)

Published OnlineFirst July 20, 2010; DOI: 10.1158/1541-7786.MCR-10-0174

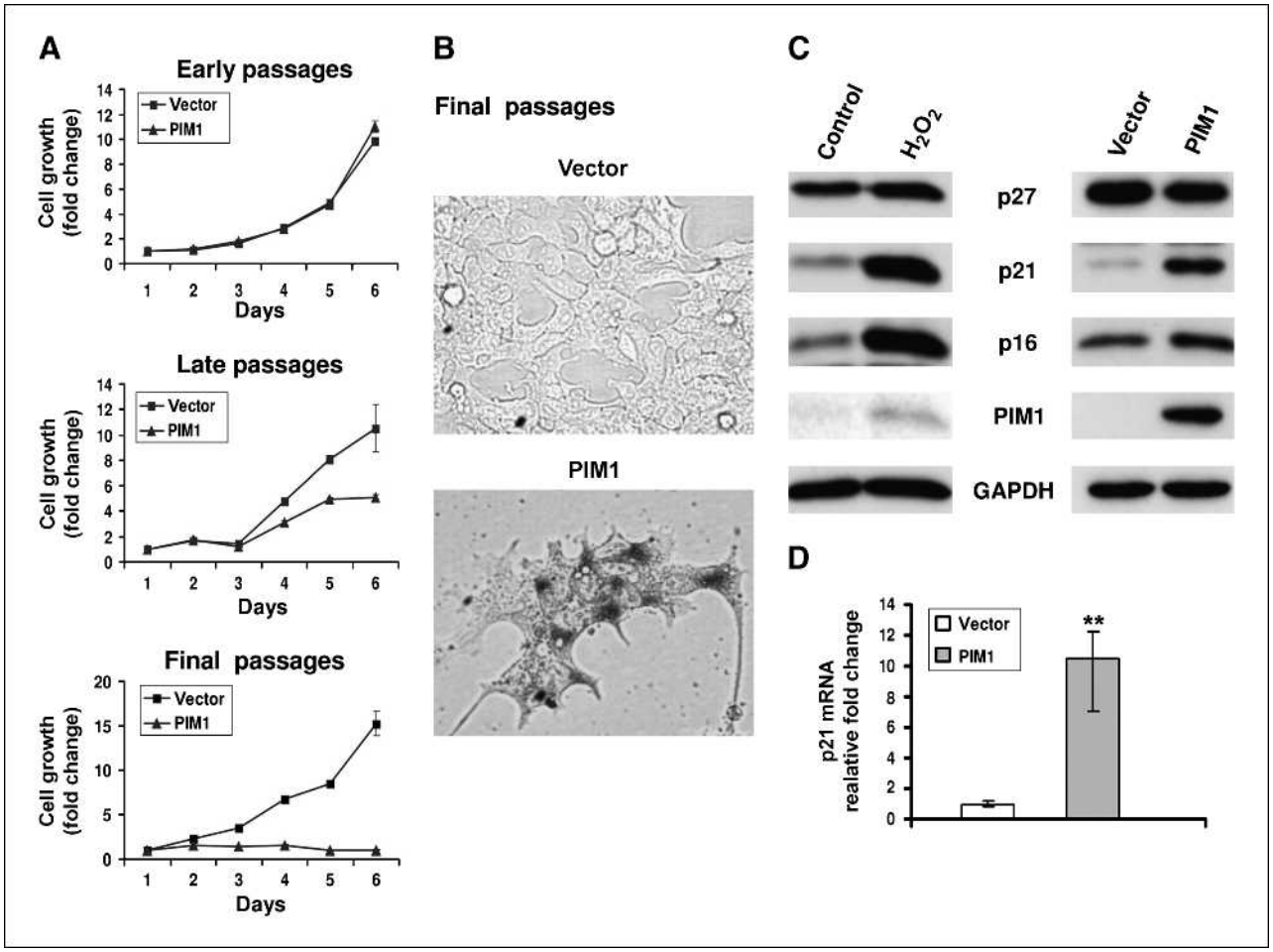

FIGURE 1. Constitutive expression of PIM1 kinase in 22Rv1 cells induces cell senescence. A, 22Rv1 cells were infected with pLNCX (vector) or pLNCX/PIM1, and pools of cells constitutively expressing PIM1 kinase were isolated. At specific cell passages, 7 to 10 (early passages), 15 to 17 (late passages), and 20 to 25 (final passages), cells were plated at equal density and assayed for cell growth (see Materials and Methods). Each point represents the mean ± SD of 12 measurements pooled from two independent experiments. B, pools of final-passage 22Rv1 cells quantitated in A were subjected to β-Gal staining. C, immunoblot analysis of 22Rv1 at passage 19 for senescence-associated markers using H_2O_2 as an inducer of cell senescence. For H_2O_2 treatment, the cells were incubated with 550 μmol/L for 2 h, H_2O_2 was removed, and 22Rv1 cells were replated and incubated in complete medium for 5 d. The measurement of GAPDH serves as a loading control. D, real-time PCR analysis of RNA collected from exponentially growing 22Rv1 vector control cells and final-passage 22Rv1 PIM1 cells studied in A and B. Each value represents the mean ± SD of nine pooled measurements produced from three independent experiments. Bars, relative fold change of RNA level from 22Rv1 PIM1 senescent cells (normalized to RNA level of the housekeeping gene GAPDH) compared with RNA level of 22Rv1 vector control cells. **, $P < 0.01$; P values were calculated by t test and represent the probability of no difference between RNA levels in vector and PIM1-expressing cells.

using the protocol described above. G418 (400 μg/mL) or hygromycin (500 μg/mL) were added to select stably infected cell populations expressing PIM1 and vector control or DN p53. After 10 days of selection, stable cell pools were established, cells were incubated in the absence or presence of doxycycline, and expression of the transgenes was verified by Western blot analysis.

To generate cells expressing PIM1 and p53 wild-type proteins, 22Rv1 stable cell lines with inducible PIM1 expression or a vector control were transfected with p53-GFP plasmid using *Trans*IT-Prostate transfection kit (Mirus) according to the manufacturer's protocol. Cells were selected with G418 (400 μg/mL) for 14 days and individual clones were isolated. Cells demonstrating GFP fluorescence were incubated with doxycycline (20 ng/mL) to induce PIM1 expression and analyzed by Western blotting for the existence of p53-GFP fusion and PIM1 proteins.

RNA interference experiments

For p21 knockdown experiments, 22Rv1 stable pools with constitutive expression of PIM1 (pLNCX/PIM1) or vector only (pLNCX) in late passage were transduced with lentiviruses encoding Tet/ON inducible control shRNA or p21 shRNA as described. Doxycycline (1 μg/mL) was added 1 day after transduction to induce the expression of shRNAs. After selection with puromycin (4 μg/mL) for 10 days, cells were pooled and analyzed.

Published OnlineFirst July 20, 2010; DOI: 10.1158/1541-7786.MCR-10-0174

Cell growth assay

To carry out the MTT assay, cells were seeded in triplicates into 96-well plates (5×10^3 per well) and allowed to adhere overnight. At the indicated times, 5 mg/mL MTT (Sigma) were added to the medium at 1:5 dilution and incubated for 3 hours; then, supernatants were removed and 100 μL DMSO per well were added to dissolve intracellular purple formazan. Absorbance was then measured at 570 nm. To measure cell growth with crystal violet (51), cells were plated in triplicates at 5×10^4 per well in 12-well plates and incubated for 10 days, fixed with 4% paraformaldehyde in PBS, and stained with 0.1% crystal violet for 20 minutes (1 mL/well). Cells were then washed three times with water and allowed to dry. The dye was then extracted from cells using 10% acetic acid, and the absorbance of this solution was measured at 590 nm.

Real-time PCR

Total RNA was extracted with the Trizol reagent (Invitrogen) and purified with acid phenol extraction. Single-stranded cDNA was constructed by Superscript III polymerase (Invitrogen) and oligo(dT) primers. Real-time PCR was performed using iCycler (Bio-Rad) and SYBR Green PCR master mix reagents (Bio-Rad). The following primers were used: p21 forward, 5′-TGGAGACTCTCAGGGTCGAAA-3′; p21 reverse, 5′-CGGCGTTTGGAGTGGTAGAA-3′; TP53INP forward, 5′-CTCATTGAACATCCCAGCATG-3′; TP53INP reverse, 5′-ATTTCATTTGCTTCCACTCTG-3′; DDIT4 forward, 5′-GCTCAGGATTTCGACTTGTTAAG-3′; DDIT4 reverse, 5′-AAACTACAAATGACTTTAGCTGACTAG-3′; IL-6 forward, 5′-AAAGAGGCACTGGCAGAAAA-3′; IL-6 reverse, 5′-TTTCACCAGGCAAGTCTCCT-3′; IL-8 forward, 5′-CTGCGCCAACACAGAAATTA-3′; IL-8 reverse, 5′-ACTTCTCCACAACCCTCTGC-3′; GAPDH forward, 5′-CAGCCTCAAGATCATCAGCA-3′; GAPDH reverse, 5′-GTCTTCTGGGTGGCAGTGAT-3′.

Senescence assays

Cells were seeded in six-well tissue culture plates (1×10^5 per well), cultured for 2 days, washed with PBS, fixed, and stained using the Senescence β-Galactosidase Staining Kit (Cell Signaling). Stained cells were visualized using a Nikon Eclipse TE 2000-S microscope under brightfield, and images were captured with Nikon Digital Camera DXM 1200F using the Q Capture software.

DNA histogram analysis

Floating and adherent cells were harvested and combined, washed with PBS, and fixed with cold 70% ethanol and stored at −20°C. The cells were then washed with PBS and resuspended in 1 mL buffer containing 100 mmol/L Tris (pH 7.4), 150 mmol/L NaCl, 1 mmol/L $CaCl_2$, 0.5 mmol/L $MgCl_2$, 0.1% NP40, 40 μg/mL RNase H, and 25 μg/mL propidium iodide. After incubation for a minimum of 30 minutes at room temperature, the cells were then analyzed with a FACScalibur flow cytometer using channel FL3.

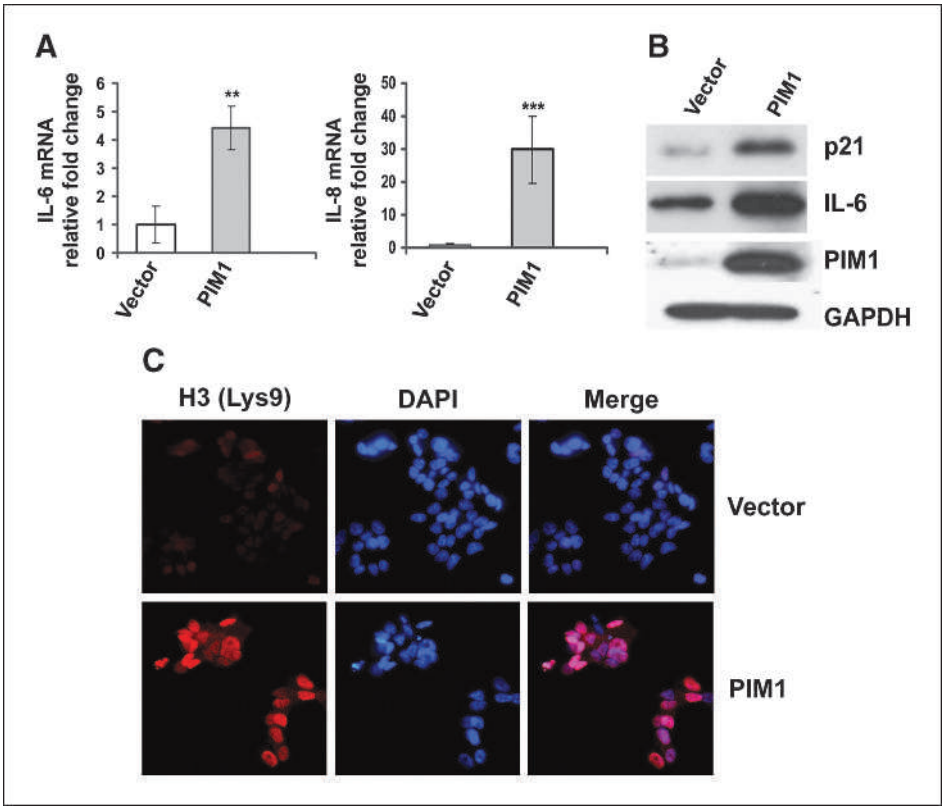

FIGURE 2. Senescence markers in 22Rv1 cells overexpressing Pim. A, as described in Fig. 1D, samples were analyzed for IL-6 and IL-8 mRNA levels. **, $P < 0.01$; P values were calculated by t test and represent the probability of no difference between RNA levels in vector and PIM1-expressing cells. ***, $P < 0.001$. B, samples from A were analyzed by Western blotting for protein expression using antibodies to the indicated proteins. GAPDH serves as a loading control. C, immunofluorescence was performed using antibodies to H3-K9m (red) for detection of SAHF foci, and 4′,6-diamidino-2-phenylindole (DAPI) staining (blue) was used to visualize DNA. Both vector and PIM1-expressing cells were at late passage (Fig. 1A).

Published OnlineFirst July 20, 2010; DOI: 10.1158/1541-7786.MCR-10-0174

Xenograft mouse models

To generate tumor xenografts, 22Rv1 early-passage cells expressing the indicated transgenes were washed twice with PBS, and the cell density was adjusted to 0.5×10^6 cells/50 μL in serum-free Dulbecco's modified Eagle's medium. An equal volume of Matrigel (BD Biosciences) was then added, and the cell suspension was injected into both the left and right dorsal flank of male Nu/nu nude mice (Charles River). On day 2 after cell implantation, doxycycline (1 μg/mL) was added into the drinking water supplemented with 5% glucose, and this solution was changed every 2nd day. Four mice carrying eight tumors were evaluated in each group. Tumor size was determined by caliper measurements, and tumor volume was calculated using the equation $(L \times W^2)/2$.

Immunostaining

Cultured 22Rv1, Cos7, or MEF cells were plated on glass coverslips into six-well plates with a density of 2×10^5 per well. The following day, cells were washed two times with PBS; fixed with 4% paraformaldehyde for 15 minutes; premeabilized with 0.1% Triton X-100 solution; and stained with IL-6, IL-8, histone H3 (Lys9), or Ki67 antibodies. For detection of centrosomes, the cells were fixed in 10% methanol. Fixed cells were incubated in blocking solution and PBS with 2% bovine serum albumin containing 2% goat serum, and immunostained with primary antibodies overnight at 4°C, followed by treatment with fluorescein isothiocyanate– or Cy3-conjugated secondary antibodies for 1 hour.

To stain tumor xenografts, these tissues were first embedded in Optimum Cutting Temperature (OCT; VWR) and frozen cryostat sections (8–10 μm) were prepared. Tissues were fixed for 7 minutes with freshly prepared 4% paraformaldehyde in PBS, permeabilized with 0.1% Triton X-100 for 30 minutes, and blocked for 30 minutes in PBS/0.1% Triton X-100/5% heat-inactivated goat serum. Sections were immunostained with anti-Ki67 antibody (1:1,000 dilution) for 1 hour, and then incubated with Cy3-conjugated secondary antibody (1:1,000 dilution) for an additional 1 hour. Fluorescence was visualized with Nikon Eclipse E800 microscope, and images were taken by Nikon digital sight DS 2 Mv camera using the NIS element BR 2.30 software.

Statistical analysis

All experiments were repeated a minimum of two times, and statistical analysis was carried out using Student's *t* test unless otherwise stated.

Results

Prostate cells constitutively expressing PIM1 kinase show irreversible inhibition of cell growth and upregulation of senescence-associated cell markers

To investigate the growth-regulatory activity of PIM1 in prostate cancer cells, we infected the human prostate cancer cell line 22Rv1 with a retrovirus expressing this cDNA, selected with G418, and collected pools of transfected cells. At increasing passage number, these cells were frozen, stored, and evaluated for their ability to grow in tissue culture (Fig. 1A). When compared with early-passage (numbers 7–10) cells, late-passage (numbers 15–17) PIM1-containing cells seemed to slow their growth. By the final passage (numbers 20–25), PIM1-expressing cells barely divided (Fig. 1B). The final-passage cells were found to have a flat and spread morphology and to be β-galactosidase (β-Gal) positive, consistent with the suggestion that they had undergone senescence (Fig. 1B). To further document the induction of the senescent phenotype by PIM1, we compared these cells to 22Rv1 cells treated with the known senescence inducer (Supplementary Fig. S1), hydrogen peroxide (H_2O_2). Increases in the protein inhibitors of cyclin-dependent kinases (31, 52, 53) are associated with the induction of senescence. Western blots show that there was no increase in the expression of the cyclin- dependent kinase inhibitor $p27^{Kip1}$ and only a moderate elevation of $p16^{INK4}$ in PIM1-containing cells compared with vector control and H_2O_2-treated cells (Fig. 1C). The level of cyclin-dependent kinase inhibitor $p21^{CIP}$ was markedly increased in both H_2O_2-treated and PIM1-expressing senescent cells, suggesting the possibility that p21 was potentially an important factor in the development of PIM1-induced senescence. The increases in p21 seemed to be transcriptionally driven as the level of mRNA for this protein was also markedly elevated (Fig. 1D). The induction of senescence by H_2O_2 also increased the amount of PIM1 protein in these tumor cells.

Cellular senescence has previously been shown to be associated with activation of a network cytokine secretion, including IL-6 and IL-8, and many proinflammatory proteins (31, 54, 55). We find that the levels of both IL-6 and IL-8 mRNA and protein are elevated in late-passage PIM1-containing cells (Fig. 2A and B and data not shown), consistent with the induction of senescence. Senescent cells accumulate stress-associated heterochromatin foci (SAHF). These heterochromatin foci are localized in the nucleus and are produced upon cellular exposure to varied stresses (31, 56). To examine whether PIM1-induced senescence correlates with SAHF formation, we performed fluorescence staining for the SAHF marker trimethyl-histone H3 (Lys9m). Our results show that late-passage cells with forced expression of PIM1 accumulated SAHF compared with vector control cells (Fig. 2C). These results show that overexpression of PIM1 kinase is capable of inducing senescence in 22Rv1 cells. In comparison, expression of PIM1 in three additional human prostate cancer cell lines, RWPE-1, RWPE-2, and Du145, neither inhibited cell growth nor induced the senescent phenotype (Supplementary Fig. S2 and data not shown). These cell lines differ from 22Rv1 cells in that they have inactive p53, whereas 22Rv1 expresses wild-type p53 protein, suggesting the possibility that p53 plays a role in regulating cellular senescence induced by PIM1 in 22Rv1 cells.

Published OnlineFirst July 20, 2010; DOI: 10.1158/1541-7786.MCR-10-0174

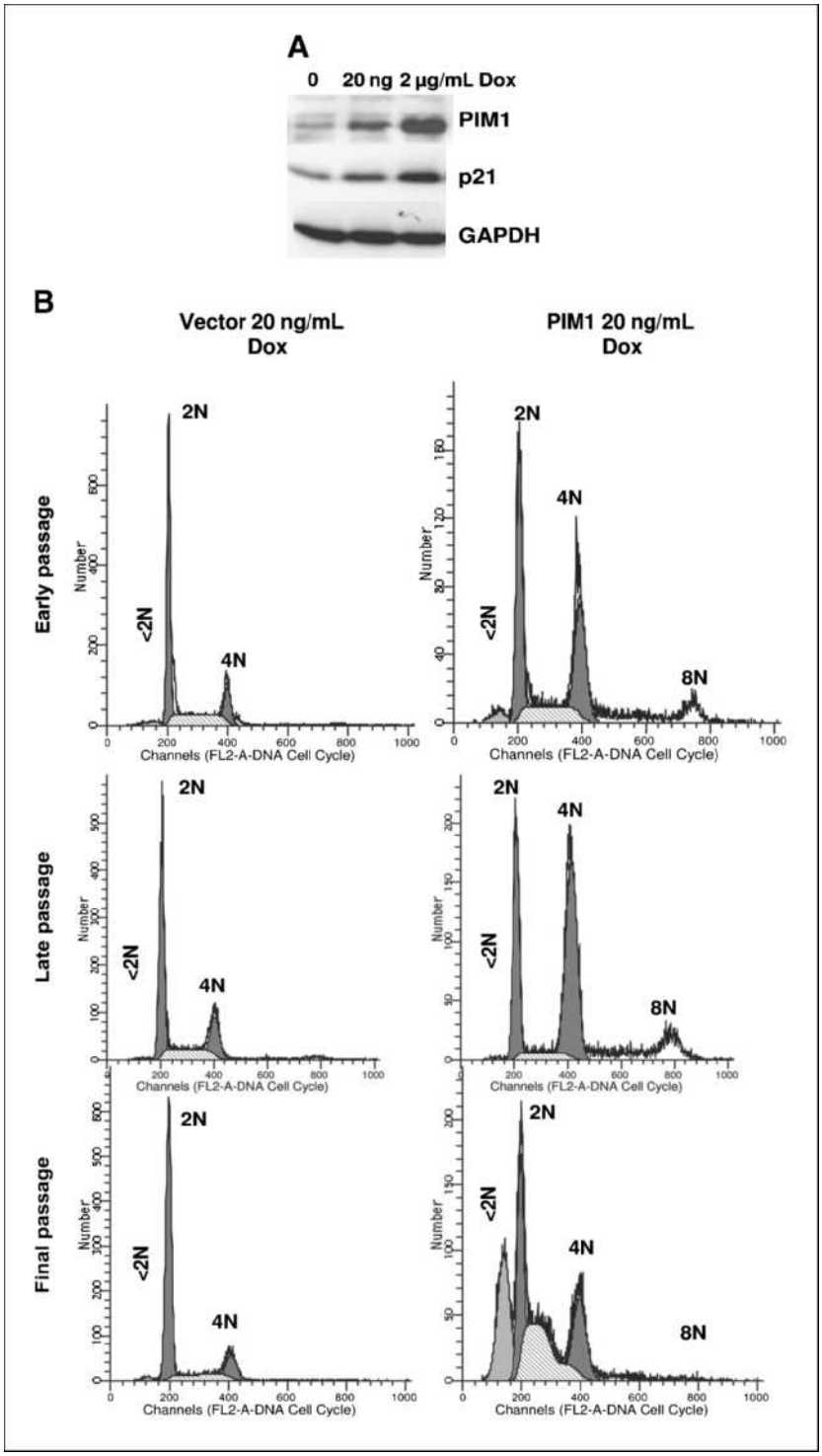

FIGURE 3. Inducible PIM1 kinase induces polyploidy and apoptosis of 22Rv1 cells in a dose- and time-dependent manner. A, immunoblot analysis of PIM1 induction and p21 expression in response to different concentrations of doxycycline (Dox). GAPDH levels serve as loading control. B, DNA histogram analysis of pTRIPz/PIM1 22Rv1 cells expressing varied PIM1 protein levels. Early-passage (8 passages), late-passage (20 passages), and final-passage (25 passages) cells were treated continuously with 20 ng/mL doxycycline. At the specified passage number, cells were pelleted and propidium iodide staining was carried out followed by FACS analysis. Less than 2N cells represent an apopotic fraction. 2N cells are diploid, 4N cells are tetraploid, and 8N cells are polyploid.

Expression of PIM1 kinase in 22Rv1 cells correlates with induction of genomic instability and apoptosis

To evaluate the ability of PIM1 protein to regulate these processes, we created 22Rv1 cell pools that contained a doxycycline-inducible PIM1 protein. These cells show that the level of PIM1 protein induced by varied doses of doxycycline correlated with the level of induction of the p21 protein (Fig. 3A). We find that the application of 20 ng/mL doxycycline to PIM1-containing cells induced a progressive time-dependent increase in both the number of cells with 4N and 8N DNA (polyploid) content as

Published OnlineFirst July 20, 2010; DOI: 10.1158/1541-7786.MCR-10-0174

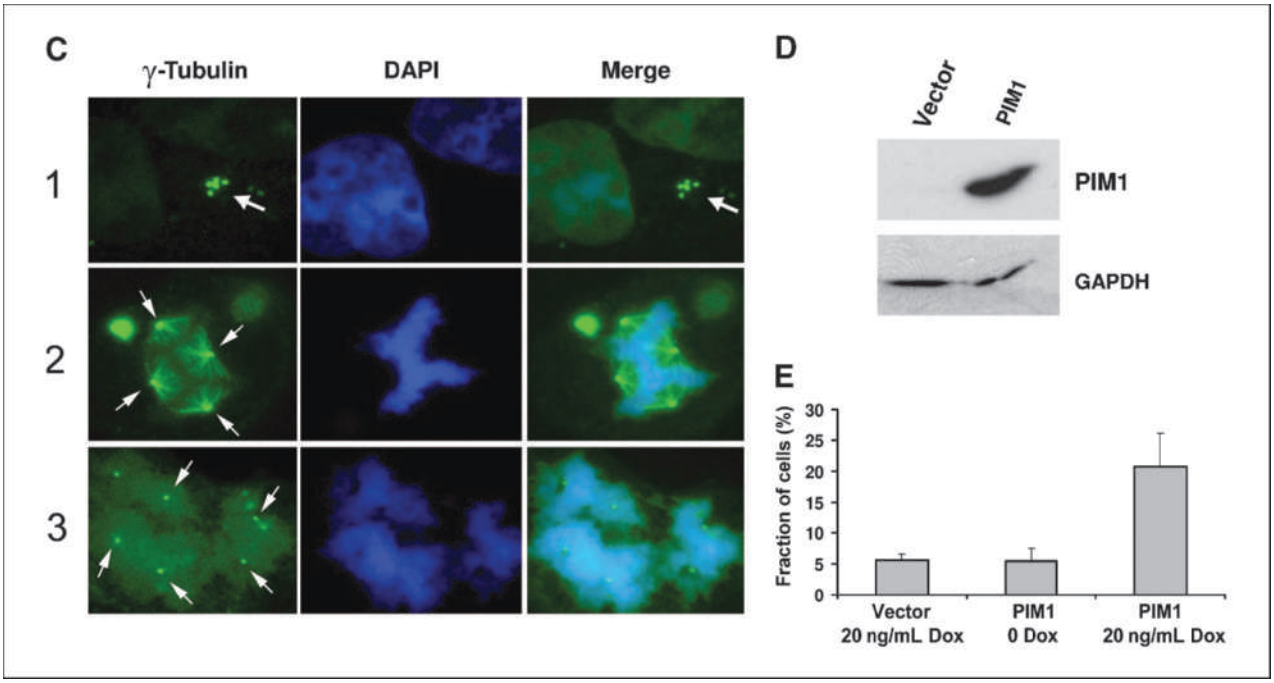

FIGURE 3 *Continued*. C, immunofluorescent images of Cos7 cells expressing inducible PIM1 kinase treated with 20 ng/mL doxycycline continuously for eight passages performed with γ-tubulin (green) antibody to visualize centrosomes and DAPI (blue) staining to visualize nuclei. Row 1 shows abnormal centrosome numbers (arrows); row 2 shows tetraploidy; and row 3 indicates Cos7 cells with multiple mitotic spindles (arrows). D, PIM1 expression in vector and PIM1 Cos7 cells at passage 8 incubated with doxycycline as in C determined by Western blotting using GAPDH as a loading control. E, fraction of cells containing more than two centrosomes per cell were measured by counting 200 cells from three independent fields. Data are presented as the mean of centrosome number ± SD.

measured by DNA histogram analysis (Fig. 3B). However, final-passage cells treated with 20 ng/mL doxycycline also showed a marked increase to ~25% in cells demonstrating <2N DNA content, consistent with the induction of apoptosis (Fig. 3B; Table 1). Treatment with higher doses of doxycycline (2 μg/mL) caused high levels of PIM1 expression and early apoptosis, and death at low passage numbers (data not shown). Additionally, to determine whether the 22Rv1 cells that constitutively expressed PIM1 studied in Figs. 1 and 2 were undergoing apoptosis, we measured the number of cells with <2N DNA content. PIM1-containing cells, but not those expressing a kinase-dead PIM1, had elevated levels of <2N cells, increased p21 expression, and showed cleavage of both poly(ADP-ribose) polymerase and β-catenin, two markers of apoptosis induction (Supplementary Fig. S4). Thus, 22Rv1 prostate cancer cells expressing elevated levels of PIM1 developed both a senescent and apoptotic phenotype.

Because 22Rv1 cells grow in clusters, making analysis of chromosome structure difficult, to document the induction of polyploidy and the potential changes in centrosome number by PIM1 overexpression, we used Cos7 cells whose morphology can be easily examined. We infected these cells with lentiviruses encoding vector only (TRIPZ) or PIM1 under the control of the doxycycline-inducible promoter. Then, we selected stable cell pools overexpressing PIM1 (Fig. 3D). Using antibodies to γ-tubulin, which stains centrosomes, passage 8 Cos7-overexpressing PIM1 cells were examined for changes in centrosome number. By counting multiple cell fields, the fraction of Cos7 cells containing more than two centrosomes in PIM1-expressing cells was found to be greater than 20% compared with 5% for control cells expressing vector alone (Fig. 3E). In this culture, cells with multiple centrosomes (row 1, arrows), tetraploid cells with four mitotic spindles (row 2, arrows), and polyploid cells with multiple centrosomes and mitotic spindles (row 3, arrows) are all visible. Although it is more difficult to identify centrosomes in fibroblasts, we repeated this experiment in embryonic fibroblasts that were isolated from mice that were genetically engineered to knock out all of the three PIM isoforms (57) and then transfected to overexpress only PIM1. γ-Tubulin staining of these cells showed the induction of multiple centrosomes (Supplementary Fig. S5).

Transition of 22Rv1/PIM1 cells to senescent phenotype is associated with DNA damage and activation of the p53 pathway

To evaluate whether the p53 pathway was activated in these PIM1-containing prostate cancer cells, we carried out quantitative reverse transcriptase-PCR (qRT-PCR) analysis of mRNA from cells expressing PIM1 at early and late passages (Fig. 1A), and examined the levels of three p53-activated genes, p53-inducible nuclear protein 1 (TP53INP1; ref. 58), DNA-damage inducible transcript 4 (DDIT4, also known as REDD1; ref. 59), and p21. We

Published OnlineFirst July 20, 2010; DOI: 10.1158/1541-7786.MCR-10-0174

found that PIM1-expressing cells at late, but not at early, passage showed marked increases in the p53-inducible genes, including TP53INP1 and DDIT4. The increase in p21 transcripts is statistically significant even at early passages but with much more dramatic effects in late-passage cells (Fig. 4A). p53 is often induced as a result of DNA damage. To document that DNA damage is occurring in PIM1-overexpressing cells, we treated the inducible cells with varying amounts of doxycycline (Fig. 4B) and then measured the levels of phosphorylated CHK2 and γH2AX, both of which are modified by double-strand DNA breaks. CHK2 is phosphorylated on Thr68 by the ATM/ATR protein kinases that are activated by double-strand DNA damage. Phosphorylation of CHK2 at Thr68 is required for subsequent activation of p53 protein in response to DNA damage (37, 60). Likewise, histone H2AX is phosphorylated on Ser139 when double-strand DNA damage occurs, yielding the γH2AX form of this histone (61, 62). A marked change in the level of phosphorylation of these proteins occurs in late-passage PIM1-containing 22Rv1 cells and mirrors increases in the levels of the p21 protein (Fig. 4B). Thus, in 22Rv1 prostate cancer cells, long-term PIM1 overexpression seems to induce polyploidy and DNA damage that is associated with the activation of p53-inducible genes, and ultimately leads to both cellular senescence and apoptosis.

Expression of DN p53 reduces polyploidy and prevents senescence and senescence-associated apoptosis in 22Rv1/PIM1 prostate cells

To evaluate whether the activation of the p53 pathway is essential for the induction of cellular senescence by PIM1, we overexpressed DN p53 in the 22Rv1 cells that contained doxycycline-inducible PIM1 and treated these cells with doxycycline (20 ng/mL). We found that in early-passage cells, DN p53 is capable of decreasing the level of the p53-inducible TP53INP-1 transcript and suppressing the induction of p21 RNA (Fig. 5A). These results are consistent with reduction of p21 protein seen by Western blotting in PIM1/DN cells (Fig. 5B). Increased levels of PIM1 kinase are known to elevate the cellular levels of cyclin B1, which can contribute to deregulation of cell division and genomic instability induced by PIM1 (63). The expression of cyclin B was gradually increased in early-passage PIM1-containing cells, but no marked changes in cyclin B1 levels was seen in PIM1/DN p53–coexpressing cells (Fig. 5B). To examine the ability of DN p53 to suppress PIM1-induced polyploidy, 22Rv1-expressing inducible PIM1 with or without DN p53 were grown in 20 ng/mL doxycycline. Early-passage cells were analyzed by DNA histogram analysis to determine the fraction expressing 8N DNA content. DN p53 suppressed the induction of the 8N cell number (Fig. 5C). To determine the effect of DN p53 on apoptosis (<2N DNA content), the same cells were grown in the presence of 20 ng/mL doxycycline and late-passage cells were studied. As shown in Fig. 5C, DN p53 was able to suppress the ability of PIM1 to induce both polyploidy and apoptosis in these prostate tumor cells. Western blots carried out on extracts of these cells showed that DN p53 suppressed both the induction of phosphorylation of the CHK2 protein kinase and γH2AX (Fig. 5D). As shown in Fig. 5D, the cyclin B1 level is markedly decreased in cells expressing high levels of PIM, and this change is reversed by the overexpression of DN p53. Finally, staining of these late-passage PIM1–overexpressing cells with β-Gal shows that blocking p53 activity also prevents the induction of this marker of cell senescence by PIM1 (Fig. 5E).

Table 1. PIM1 kinase induces polypoidy and apoptosis in 22Rv1 cells

	20 ng/mL Dox	
	Vector	**PIM1**
Early		
<2N	0.727%	0.54%
2N	63.56%	33.63%
4N	15.42%	39.69%
>4N	0.81%	14.78%
Late		
<2N	1.37%	1.61%
2N	65.39%	15.30%
4N	9.82%	46.95%
>4N	1.66%	27.72%
Final		
<2N	3.46%	25.71%
2N	70.86%	33.71%
4N	13.30%	13.57%
>4N	1.62%	4.99%

NOTE: Values in table are representative values obtained from triplicate experiments.
Abbreviation: DOX, doxycycline.

Expression of DN p53 restores the ability of 22Rv1/PIM1 cells to grow as tumors

To examine the ability of DN p53 to regulate 22Rv1 tumor growth driven by PIM1, these cells were injected into the flanks of nude mice and the animals were treated with doxycycline in water. On day 27, tumor size was measured and the animals were sacrificed. In comparison to vector, PIM1-containing 22Rv1 tumors grew poorly, and this decreased growth was completely reversed by the overexpression of DN p53. In addition, the tumors coexpressing PIM1 and DN p53 showed a slight statistical increase in growth compared with vector control. Western blots carried out on tumor extracts showed a lower level of p21 protein and a decreased phosphorylation of CHK2 and γH2AX in DN p53–expressing tumors when compared with those expressing PIM1 (Fig. 6). Consistent with these results and the slow growth of the tumors, staining of PIM1-containing tumors showed low levels of cell division, as measured by the proliferation marker Ki67, and stained positively for senescence-associated β-galactosidase (SA-β-Gal). Both of these changes were reversed by DN p53

Published OnlineFirst July 20, 2010; DOI: 10.1158/1541-7786.MCR-10-0174

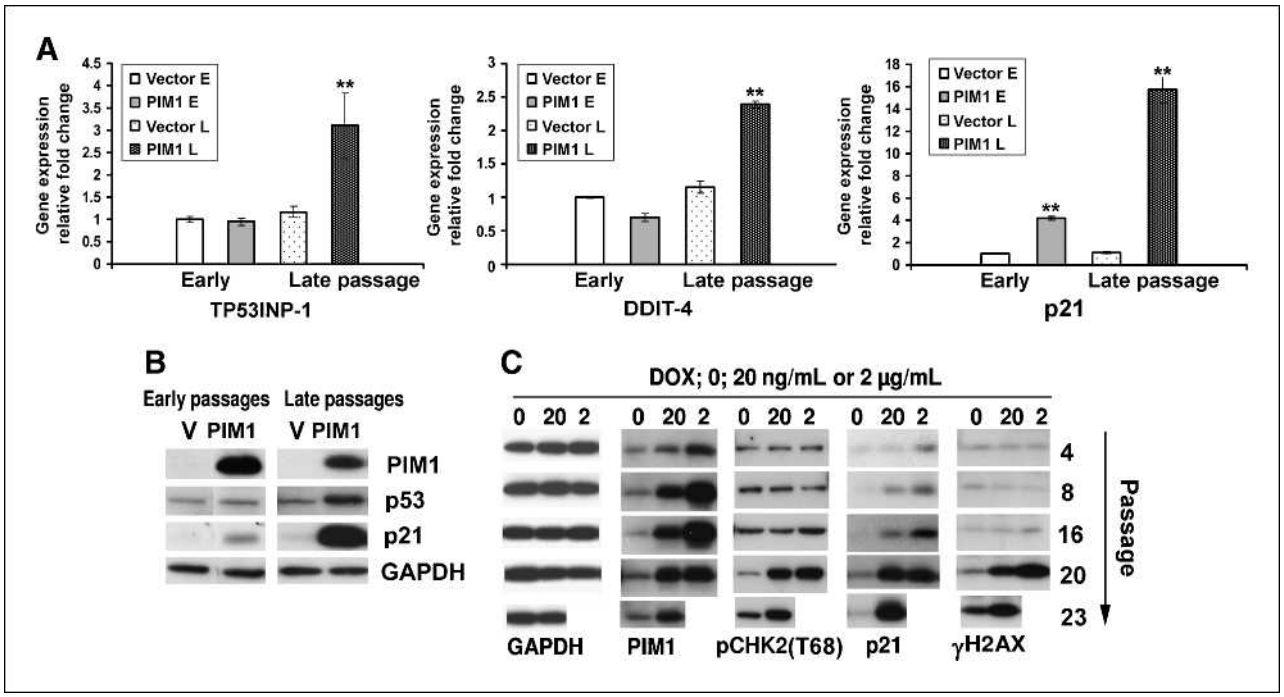

FIGURE 4. Transition of 22Rv1/PIM1 cells to senescent phenotype is associated with activation of the p53 pathway and a DNA damage signaling response. A, stable pools of prostate 22Rv1 constitutively expressing PIM1 or vector in early and final passages, as shown at Fig. 1A and Supplementary Fig. S4, were subjected to gene expression analysis by qRT-PCR. mRNA levels are represented relative to those found in vector control cells. Each value represents the mean ± SD of six pooled measurements produced from two independent experiments. **, $P < 0.01$; P values were calculated by t tests and represent the probability of no difference between mRNA levels in vector and PIM1-expressing cells. B, 22Rv1 cells in early (4, 8, 16) and late (23, 25) passages with differential levels of PIM1 expression (see Fig. 3) were (C) induced by the indicated concentrations of doxycycline (0, 20 ng/mL, or 2 μg/mL) and were analyzed by immunoblotting for PIM1, phosphorylated CHK2 (Thr68), p21, and γH2AX protein levels. GAPDH serves as loading control.

overexpression. Cells isolated from these tumors and placed back into culture behaved similarly to the tumors (Supplementary Fig. S5) with predictable changes in protein levels (Supplementary Fig. S5A), Ki-67 (Supplementary Fig. S5B), and SA-β-Gal (Supplementary Fig. S5C).

Activation of p53 inhibits cell growth and increases cell senescence in 22Rv1 cells expressing PIM1

The observation that DN p53 blocks PIM1-induced senescence suggested the possibility that activation or overexpression of p53 would enhance the induction of these cellular changes. To further define the role of p53 in PIM1-induced senescence, 22Rv1 cells containing inducible PIM1 were transfected with p53 and doubly expressing clones were selected with G418. Comparison of the growth of 22Rv1 cells expressing p53, PIM1, or both proteins showed that PIM1 expression alone did not inhibit the growth of cells on tissue culture–coated plates, whereas p53 had a modest inhibitory effect, and the simultaneous overexpression of both proteins causes significant growth inhibition (Fig. 7A). This result is clearly seen when p53 and p53/PIM1 22Rv1 cells are allowed to grow for 10 days in tissue culture, and then fixed and stained with crystal violet (Fig. 7B). This inhibition in cell growth could result from the effect of PIM1 and p53 on elevating the levels of p21 (Fig. 7C). Also, when PIM1 and p53 were expressed simultaneously, β-Gal staining of these cell lines revealed significantly increased levels of cell senescence (Fig. 7D).

Knockdown of p21 expression rescues cells from senescence

The Cdk inhibitor p21 was first identified as an overexpressed marker in senescent cells and later found to be capable of regulating senescence in both normal and cancer cells. p21 mediates, in part, the effects of p53, although other genes are also involved (for review, see ref. 64) in the p53-induced biological changes. To examine the role of p21 in these cells, lentiviral vectors were used to transduce a Tet/ON-inducible shRNA directed at p21 (sh-p21) or a control sequence (sh-c) into 22Rv1 cells constitutively expressing PIM1 or a control vector. This shRNA was successful in decreasing p21 levels in control and PIM1-containing cells (Fig. 8B), but had no effect on the growth of 22Rv1 cells (Fig. 8A). In contrast, the growth of PIM1-containing 22Rv1 cells was markedly stimulated (Fig. 8A) by decreasing the p21 levels. In these cells, decreased p21 levels correlated with a markedly lower level of γ-H2AX (Fig. 8B), suggesting that cells containing lower p21 levels showed a decreased level of DNA damage. In addition, lower levels of p21 protein in PIM1-containing cells correlated with a marked decrease in SA-β-Gal staining and an inhibition in the induction of the senescence phenotype.

Published OnlineFirst July 20, 2010; DOI: 10.1158/1541-7786.MCR-10-0174

Discussion

The current study shows that PIM1 kinase can induce cellular senescence in prostate carcinoma cells 22Rv1 based on (*a*) irreversible inhibition of cell proliferation accompanied by decreasing Ki-67 staining, (*b*) formation of β-Gal–positive cells both in culture and in xenograft models, (*c*) elevation in the mRNA and protein levels of IL-6 and IL-8, and (*d*) SAHP-positive staining. PIM1-induced senescence has been previously reported in primary normal MEFs (23). The induction of senescence by PIM1 seems to depend on an intact p53-p21 pathway. PIM1 induced senescence in 22Rv1 cells that are p53 wild type, whereas prostate cell lines, including PC3, Du145, RWPE-1, and RWPE-2, which contain a mutant, deleted, or inactivated p53 gene grow with high levels of PIM1 and avoid senescence. Additional evidence pointing to the importance of p53 in PIM-induced senescence includes the observation that DN p53 protein blocks the PIM1-induced senescence in culture, and that in mouse xenograft models (Figs. 5 and 6; Supplementary Fig. S5), the knockdown of p21 mRNA markedly enhances cell growth and decreases the number

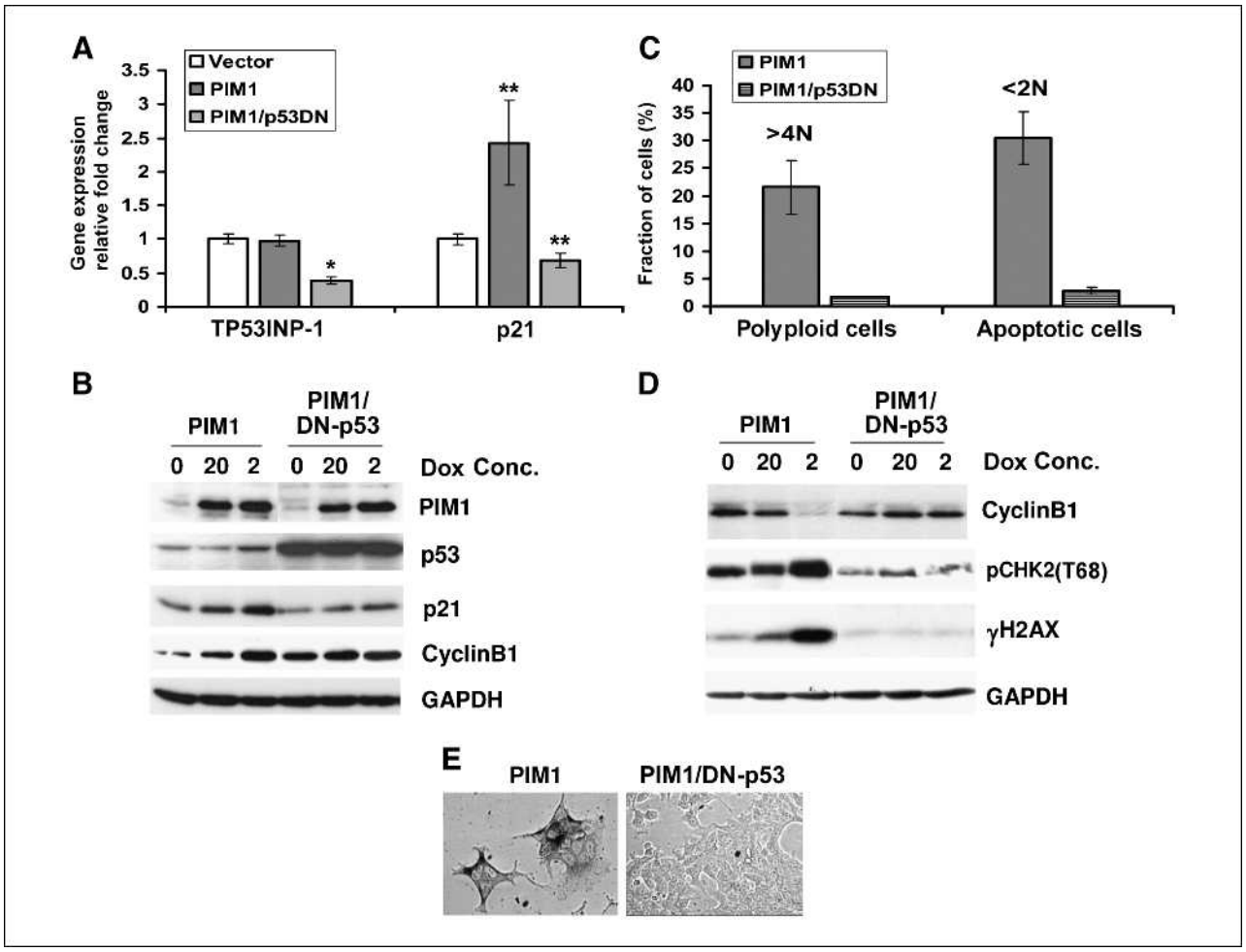

FIGURE 5. Expression of DN p53 reduces PIM1-induced polyploidy and prevents cellular senescence in 22Rv1/PIM1 prostate cells. A, inducible 22Rv1/PIM1 cells were infected with retroviruses encoding DN p53, and stable pools were maintained in 2 μg/mL doxycycline. To examine mRNA changes, early-passage cells were analyzed by qRT-PCR to determine the levels of the p53 transcriptional targets TP53INP and p21. The levels of mRNA are represented relative to those found in vector control cells. Each value represents the mean ± SD of six pooled measurements produced from two independent experiments. **, $P < 0.01$; P values were calculated by t tests and represent the probability of no difference between RNA levels in vector and PIM1 or PIM1/DN p53–expressing cells. B, cells analyzed in A were assessed by immunoblotting for protein expression as indicated. The cells were treated with the following doxycycline concentrations: 0, 20 ng, and 2 μg/mL. A Western blot for GAPDH serves as loading control. C, a bar graph quantitating the number of cells with <2N and >4N DNA content in 22Rv1 cells expressing PIM1 or PIM1/DN p53. The number of polyploid cells (>4N) was derived from early-passage cells, whereas the number of apoptotic cells (<2N) came from cells that are in late passages. Cells were incubated in the presence of 20 ng/mL doxycycline, and DNA histograms were analysed by flow cytometry. The *Y* axis represents the percentage of cells with DNA content less than 2N (apoptotic population) or with DNA content more than 4N (polyploid population). Each point represents the mean ± SD of data pooled from three independent experiments. D, late-passage 22Rv1/PIM1 and PIM1/DNp53 cells were examined by immunoblotting for the levels of specific protein. The doxycycline concentrations used for the induction of PIM1 expression were the same as in B. GAPDH levels serve as a loading control. E, 22Rv1 cells studied in D were analyzed for β-Gal expression.

Published OnlineFirst July 20, 2010; DOI: 10.1158/1541-7786.MCR-10-0174

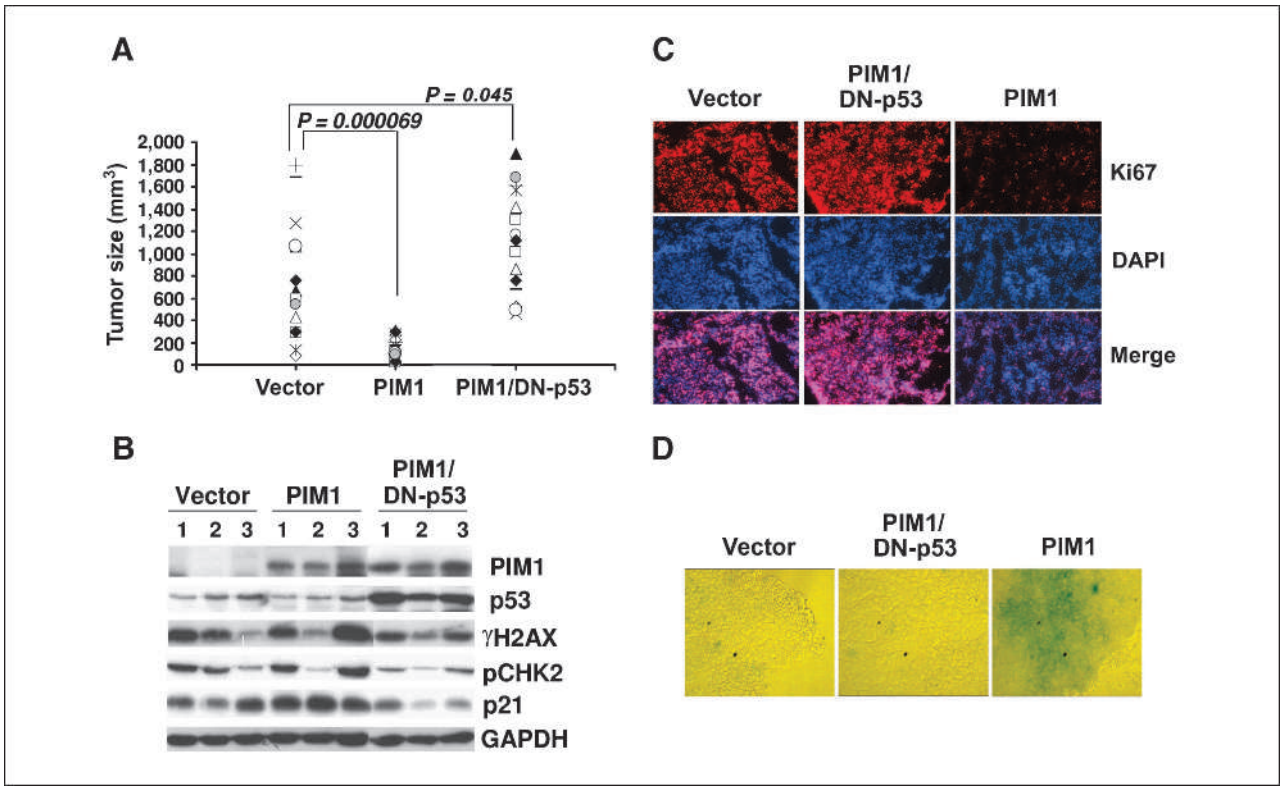

FIGURE 6. Expression of DN p53 enhances tumor growth of 22Rv1/PIM1 cells. A, male Nu/nu mice were injected subcutaneously with 0.5×10^6 22Rv1vector control, 22Rv1/PIM1, or 22Rv1/PIM1/DN p53 cells on both the left and right flanks. Twenty-four hours later, 1 μg/mL doxycycline was added in the drinking water. Tumor sizes were measured before sacrificing the mice on day 27. Data shown are from two independent experiments (16 tumors for each cell line) and represent the mean tumor volume. *P* values were calculated using Mann-Whitney statistical analysis. B, lysates from three different tumors from each group were analyzed by immunoblotting for expression of the indicated proteins. C, frozen sections from 22Rv1vector control, 22Rv1/PIM1, or 22Rv1/PIM1/DN p53 were fixed and immunostained for the proliferation marker Ki67 (red in the overlay). DAPI staining (blue in the overlay) was used to visualize DNA. Data represent one section from each of three tumors analyzed. D, frozen sections of 22Rv1/vector, 22Rv1/PIM1, and 22Rv1/PIM1/DN p53 tumors were stained with β-Gal.

of β-Gal–positive cells (Fig. 8). Our observation that ectopically expressed p53 induces cell growth arrest and increases the number of β-Gal–positive cells in 22Rv1/PIM1 cells compared with vector control (Fig. 7) also suggests that the activation of p53 pathway is capable of enhancing the PIM1-induced senescence response. Because PIM1 does not upregulate p27 (Fig. 1C), a protein critical to the induction of senescence by AKT1 in prostate cells (52), it is likely that the mechanism by which these protein kinases function to induce senescence is markedly different.

The control of PIM1 protein expression levels in tumors is complex and is regulated at the transcriptional (65, 66) and translational levels by specific microRNAs (67). Pim expression is controlled posttranslationally by modifications such as ubiquitination and protein dephosphorylation (68, 69). Quantitative expression of PIM1 measured by qRT-PCR reveals 2.75-fold and 4.45-fold increase of PIM1 mRNA in benign prostatic hyperplasia and in prostate cancer, respectively, when compared with PIM1 mRNA levels in normal prostate (21, 70). These data suggest that PIM1 overexpression is likely an early event in prostate carcinogenesis. We find that PIM1 expression is also capable of inducing apoptosis in a p53-dependent manner, and the time course of induction of cell death seems related to the level of PIM1 in these tumor cells. In a breast cancer cell model driven by oncogenes, apoptosis and senescence have been shown to occur simultaneously in one culture (71). The reason why a cell chooses to undergo apoptosis versus senescence is complex and not fully understood. The extent and persistence of DNA damage may play a major role in regulating both of these phenotypes (35). Alternatively, overexpression of antiapoptotic molecules, such as BCL-2 or transcription factors CREB and SLUG (28, 72-74), may enhance the induction of senescence. Factors that modulate growth arrest versus senescence include cofactors for p53-mediated transcriptional activation, including the BRN-3a protein that induces senescence over apoptosis. The DAXX protein can function to inhibit p21 without regulating p53 to influence the induction of proapoptotic genes (75-77).

Consistent with its activation of p53, our results indicate that PIM1 induces 3-fold increase in p21 mRNA level in early-passage cells and a marked 12- to 16-fold increase in the levels of the p21 transcript when PIM1-expressing prostate cancer cells undergo senescence (Figs. 1D and 4A). Previous data showed that PIM1 phosphorylates p21 protein on

Published OnlineFirst July 20, 2010; DOI: 10.1158/1541-7786.MCR-10-0174

Thr145 and on Ser146, thus promoting p21 protein stabilization in p53-null H1299 lung carcinoma cells (78). Because the expression of DN p53 decreased the level of p21 protein in this model, we suggest that the elevation of p21 protein is largely driven by increased transcription of the p21 mRNA and not by changes in protein stability (Fig. 5). It cannot be ruled out that in early-passage cells where major DNA damage has not taken place, small changes in p21 levels could be regulated by protein stability. We find that in early-passage 22Rv1 cells that express relatively large amounts of PIM1, there was no highly significant change in p53 protein levels and no induction of the p53 target genes TP53INP-1 and DDIT-4 (Fig. 4A). It is possible that small changes in p53 levels activated by PIM1 stabilization of the Mdm2-ARF complex (23) could be driving increases in transcription of p21, or, as our earlier work suggested (79), that other signaling pathways (i.e., PKC) possibly regulated by PIM1 could be playing a role in modulating p21 mRNA levels.

The DNA damage signaling pathway connects cellular stresses to cellular senescence (80). We analyzed the DNA damage response in 22Rv1 PIM1-expressing cells by measuring phosphorylation of CHK2 and the minor histone H2AX (Fig. 4C). In response to DNA damage, H2AX becomes phosphorylated on Ser139 and CHK2 on Thr68 by ATM (37, 60, 62). Early-passage cells do not induce changes in these two proteins; however, in late-passage cells, both CHK2 phosphorylation and γH2AX expression are markedly increased (Fig. 4B). Because CHK2 can phosphorylate and activate p53, these changes explain in part the temporal relationship between PIM1-dependent DNA damage and the activation of the p53 pathway leading to transcription of downstream genes (e.g., DDIT4; ref. 59). OIS has been

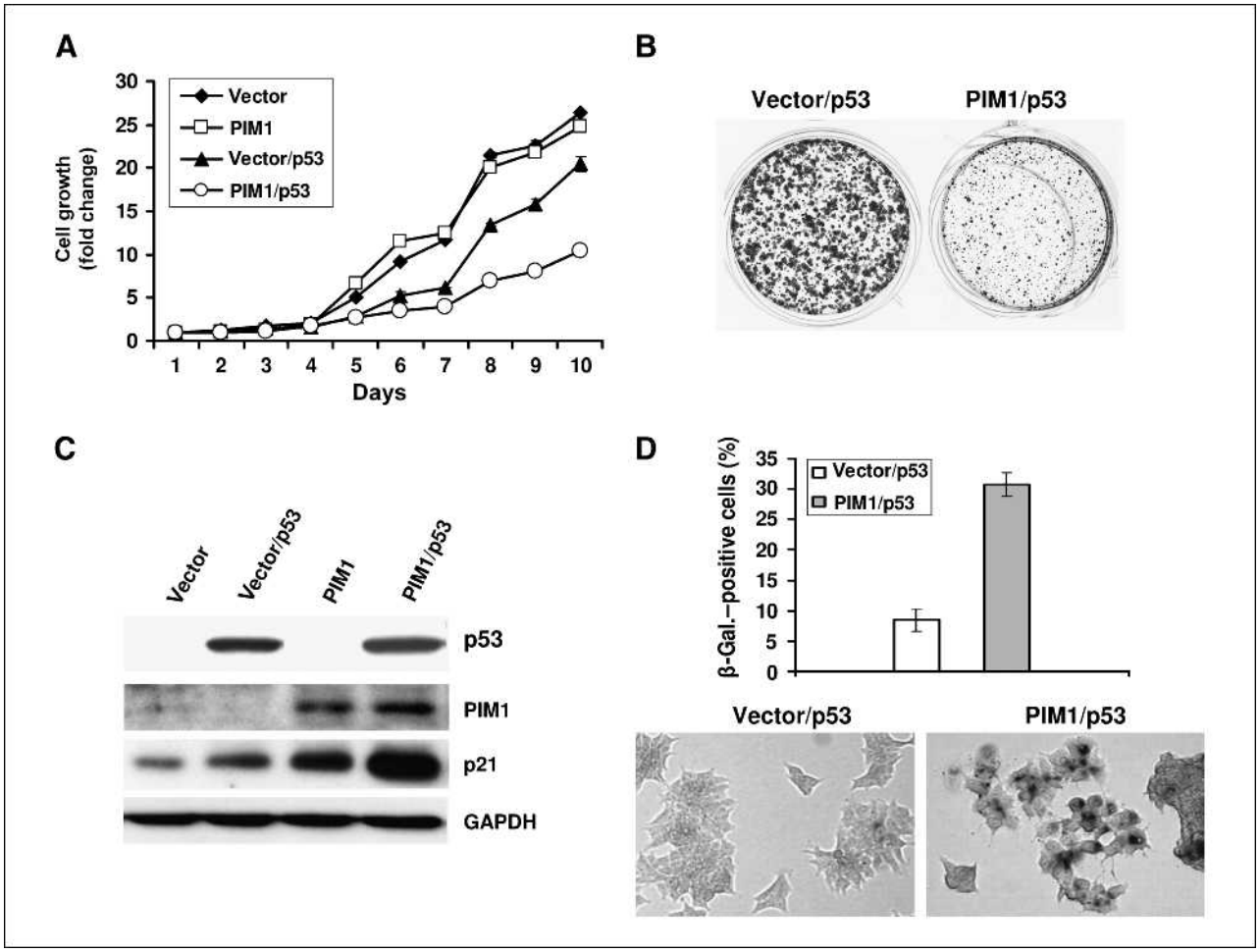

FIGURE 7. Coexpression of p53 and PIM1 proteins inhibits cell growth and increases cell senescence. Early-passage 22Rv1/vector and 22Rv1/PIM1 doxycycline-inducible stable cell lines were transfected with a plasmid encoding wild-type p53-GFP. Cells were selected with G418 (400 μg/mL) and grown in the presence of doxycycline (20 ng/mL) to induce PIM1 expression. Two clones positive for p53 from each cell type were pooled and analyzed. A, cells were plated with equal density, and cell growth was measured using the crystal violet assay described in Materials and Methods. Each point represents the mean ± SD of six independent measurements. B, cells were plated at equal density, allowed to grow for 10 d, and then fixed and stained with crystal violet. C, extracts of 22Rv1 cells containing p53, PIM1, or both were assayed for p21 protein levels as determined by immunoblotting with the specified antibodies. The level of GAPDH protein serves as a loading control. D, cells were stained for β-Gal. The percentage of β-Gal–positive cells was calculated from the observation of 200 cells in three independent fields. Data presented are the mean ± SD of three independent experiments.

Published OnlineFirst July 20, 2010; DOI: 10.1158/1541-7786.MCR-10-0174

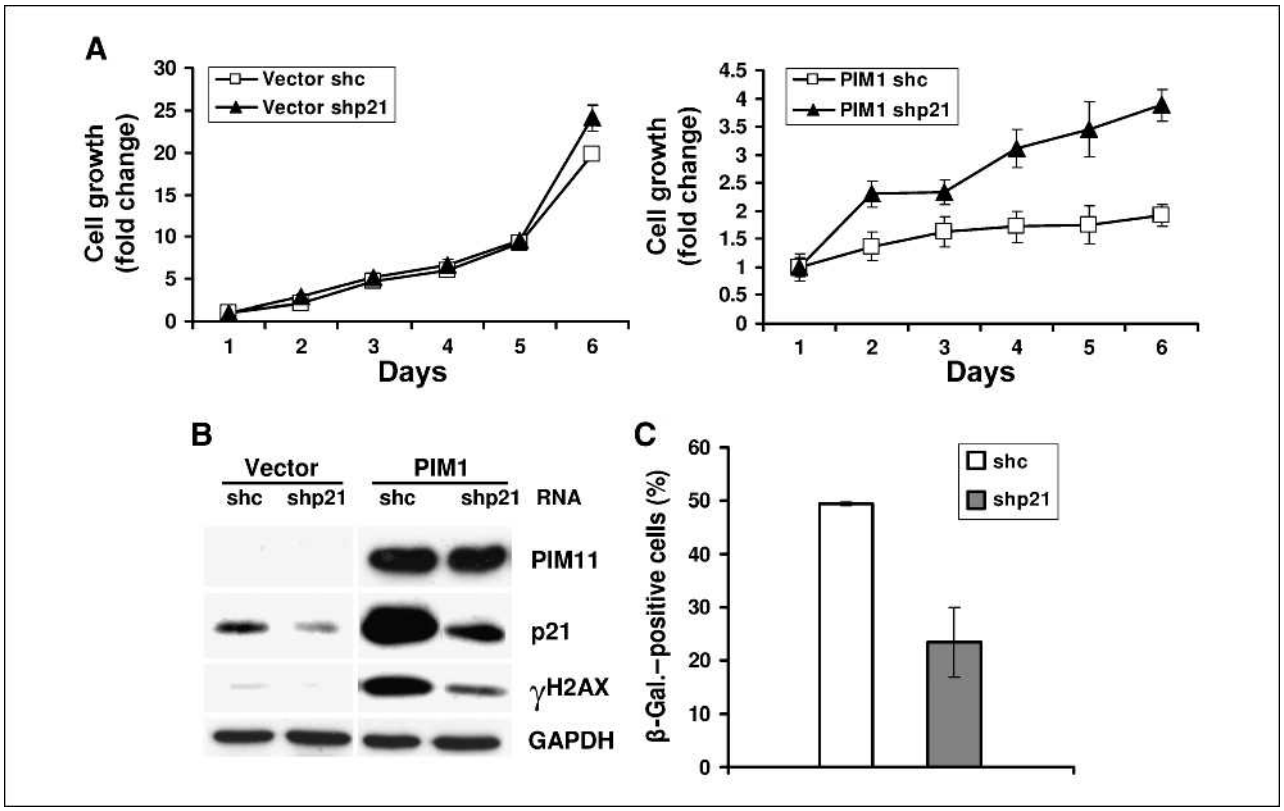

FIGURE 8. Knockdown of p21 expression with shRNA rescues cells from senescence. In passage 15, prostate 22Rv1/pLNCX (vector) cells and 22Rv1/PIM1 (PIM1) cells constitutively expressing PIM1 kinase were infected with lentiviruses encoding control shRNA (shc) or p21 shRNA (shp21) under control of Tet/ON promoter. Cells were treated with puromycin (4 μg/mL), and doxycycline (1 μg/mL) was added on the 2nd day after infection to induce expression of shRNAs. A, cells were plated with equal density and allowed to grow for 6 d. Cell growth was analyzed by the MTT assay. Each point represents the mean ± SD of six measurements. Results from one of three independent experiments are graphed. B, samples from A were analyzed by immunobloting for expression of PIM1, p21, and γH2AX protein levels with GAPDH serving as loading control. C, the cells from A were stained for β-Gal, and the number of positive cells out of 200 cells counted in three independent fields was graphed. Data are presented as the mean ± SD from three replicate experiments.

linked to DNA replicative stress, possibly through the induction of reactive oxygen species (81, 82) marked by aberrant premature termination of replication fork progression, leading DNA breakage, DNA damage response, and induction of senescence (34, 83). Genomic instability and DNA damage have been observed in both early human precancerous lesions and tumors, and this instability is closely related with induction of DNA damage response (84). Recent data also showed that PIM1 kinase plays a central role in DNA damage–evoked neuronal death by regulating aberrant neuronal cell cycle activation (85). Our results (Fig. 3; Supplementary Fig. S4), and data from others (86, 87), identify defects in mitotic spindle checkpoint, centrosome amplification, and chromosome misaggregation, resulting in the appearance of aneuploidy and polyploidy in PIM1-overexpressing cells. The mechanism by which PIM1 induces these changes is unclear. Increases in cyclin B1 expression in the early passage of 22Rv1/PIM1 cells could possibly contribute and have been identified in other cell lines (Fig. 5; ref. 63). During mitosis, PIM1 has been shown to be located in the spindle poles in complex with NuMA, HP1β, dinein, and dynactin, suggesting that the PIM1 kinase might regulate the mitotic apparatus (88).

A model describing the findings of the present study can be summarized as follows: PIM1 induces chromosomal and genomic instability followed by DNA damage and p53 activation, which in turn enhances p21 expression; these cellular changes then lead to senescence. The 22Rv1 cell line originated from primary human carcinoma that shows significant genetic drift caused by microsatellite instability compared with other human prostate carcinoma cell lines (89). The additional genomic instability induced by PIM1 expression enhances DNA damage response and p53 activation, leading to senescence in 22Rv1 cancer cells. Thus, for PIM to enhance tumor growth and progression, two cellular changes are critical (*a*) baseline genomic instability and (*b*) inactivation of the p53 pathway, allowing these tumor cells to bypass the induction of cellular senescence and apoptosis.

Small-molecule inhibitors of the PIM protein kinases have been described (for review, see ref. 90) and are targeted for the treatment of prostate cancer, leukemia, and lymphoma. Our studies suggest that tumors that develop elevated PIM kinase levels will most likely have a defective p53 pathway. Thus, the ability to induce cellular apoptosis

Published OnlineFirst July 20, 2010; DOI: 10.1158/1541-7786.MCR-10-0174

by targeting PIM1 alone may be compromised by the absence of a robust p53 response.

Disclosure of Potential Conflicts of Interest

No potential conflicts of interest were disclosed.

Acknowledgments

We thank Margaret Romano [Pathology and Laboratory Medicine at the Medical University of South Carolina (MUSC)] for preparation of frozen sections from tumor xenografts, Richard M. Peppler (Hollings Cancer Center at MUSC) for flow cytometry analysis, and Pamela A. Knox (Hollings Cancer Center) for technical assistance in the preparation of the manuscript. Dr. Carola Neumann (MUSC) kindly provided the DN p53 plasmid, and Dzmitry Fedorovich (MUSC) helped in the creation of the 22Rv1 cells coexpressing PIM1 and wild-type p53 proteins. We thank Dr. Anton Berns (The Netherlands Cancer Institute) for the PIM knockout mice.

Grant Support

Department of Defense grant W8IXWH-08. The flow cytometry shared resource was funded by 2P30-CA138313.

The costs of publication of this article were defrayed in part by the payment of page charges. This article must therefore be hereby marked *advertisement* in accordance with 18 U.S.C. Section 1734 solely to indicate this fact.

Received 04/23/2010; revised 06/15/2010; accepted 07/02/2010; published OnlineFirst 07/20/2010.

References

1. Cuypers HT, Selten G, Quint W, et al. Murine leukemia virus-induced T-cell lymphomagenesis: integration of proviruses in a distinct chromosomal region. Cell 1984;37:141–50.
2. Selten G, Cuypers HT, Berns A. Proviral activation of the putative oncogene Pim-1 in MuLV induced T-cell lymphomas. EMBO J 1985;4:1793–8.
3. Selten G, Cuypers HT, Boelens W, et al. The primary structure of the putative oncogene pim-1 shows extensive homology with protein kinases. Cell 1986;46:603–11.
4. van Lohuizen M, Verbeek S, Krimpenfort P, et al. Predisposition to lymphomagenesis in pim-1 transgenic mice: cooperation with c-myc and N-myc in murine leukemia virus-induced tumors. Cell 1989;56:673–82.
5. Ellwood-Yen K, Graeber TG, Wongvipat J, et al. Myc-driven murine prostate cancer shares molecular features with human prostate tumors. Cancer Cell 2003;4:223–38.
6. Hammerman PS, Fox CJ, Birnbaum MJ, Thompson CB. Pim and Akt oncogenes are independent regulators of hematopoietic cell growth and survival. Blood 2005;105:4477–83.
7. Zippo A, De Robertis A, Serafini R, Oliviero S. PIM1-dependent phosphorylation of histone H3 at serine 10 is required for MYC-dependent transcriptional activation and oncogenic transformation. Nat Cell Biol 2007;9:932–44.
8. Wang J, Kim J, Roh M, et al. Pim1 kinase synergizes with c-MYC to induce advanced prostate carcinoma. Oncogene 2010;29:2477–87.
9. van Kreijl CF, van der Houven van Oordt CW, Kroese ED, Sorensen IK, Breuer ML, Storer RD. Evaluation of the Emu-pim-1 transgenic mouse model for short-term carcinogenicity testing. Toxicol Pathol 1998;26:750–6.
10. van der Houven van Oordt CW, Schouten TG, van Krieken JH, van Dierendonck JH, van der Eb AJ, Breuer ML. X-ray-induced lymphomagenesis in E mu-pim-1 transgenic mice: an investigation of the co-operating molecular events. Carcinogenesis 1998;19:847–53.
11. Dhanasekaran SM, Barrette TR, Ghosh D, et al. Delineation of prognostic biomarkers in prostate cancer. Nature 2001;412:822–6.
12. Valdman A, Fang X, Pang ST, Ekman P, Egevad L. Pim-1 expression in prostatic intraepithelial neoplasia and human prostate cancer. Prostate 2004;60:367–71.
13. Hsi ED, Jung SH, Lai R, et al. Ki67 and PIM1 expression predict outcome in mantle cell lymphoma treated with high dose therapy, stem cell transplantation and rituximab: a Cancer and Leukemia Group B 59909 correlative science study. Leuk Lymphoma 2008;49:2081–90.
14. Wallentine JC, Kim KK, Seiler CE III, et al. Comprehensive identification of proteins in Hodgkin lymphoma-derived Reed-Sternberg cells by LC-MS/MS. Lab Invest 2007;87:1113–24.
15. Amson R, Sigaux F, Przedborski S, Flandrin G, Givol D, Telerman A. The human protooncogene product p33pim is expressed during fetal hematopoiesis and in diverse leukemias. Proc Natl Acad Sci U S A 1989;86:8857–61.
16. Beier UH, Weise JB, Laudien M, Sauerwein H, Gorogh T. Overexpression of Pim-1 in head and neck squamous cell carcinomas. Int J Oncol 2007;30:1381–7.
17. Peltola K, Hollmen M, Maula SM, et al. Pim-1 kinase expression predicts radiation response in squamocellular carcinoma of head and neck and is under the control of epidermal growth factor receptor. Neoplasia 2009;11:629–36.
18. Reiser-Erkan C, Erkan M, Pan Z, et al. Hypoxia-inducible proto-oncogene Pim-1 is a prognostic marker in pancreatic ductal adenocarcinoma. Cancer Biol Ther 2008;7:1352–9.
19. Babel I, Barderas R, Diaz-Uriarte R, Martinez-Torrecuadrada JL, Sanchez-Carbayo M, Casal JI. Identification of tumor-associated autoantigens for the diagnosis of colorectal cancer in serum using high density protein microarrays. Mol Cell Proteomics 2009;8:2382–95.
20. Cibull TL, Jones TD, Li L, et al. Overexpression of Pim-1 during progression of prostatic adenocarcinoma. J Clin Pathol 2006;59:285–8.
21. He HC, Bi XC, Zheng ZW, et al. Real-time quantitative RT-PCR assessment of PIM-1 and hK2 mRNA expression in benign prostate hyperplasia and prostate cancer. Med Oncol 2009;26:303–8.
22. Chen WW, Chan DC, Donald C, Lilly MB, Kraft AS. Pim family kinases enhance tumor growth of prostate cancer cells. Mol Cancer Res 2005;3:443–51.
23. Hogan C, Hutchison C, Marcar L, et al. Elevated levels of oncogenic protein kinase Pim-1 induce the p53 pathway in cultured cells and correlate with increased Mdm2 in mantle cell lymphoma. J Biol Chem 2008;283:18012–23.
24. Xu M, Yu Q, Subrahmanyam R, Difilippantonio MJ, Ried T, Sen JM. β-Catenin expression results in p53-independent DNA damage and oncogene-induced senescence in prelymphomagenic thymocytes *in vivo*. Mol Cell Biol 2008;28:1713–23.
25. Ristriani T, Fournane S, Orfanoudakis G, Trave G, Masson M. A single-codon mutation converts HPV16 E6 oncoprotein into a potential tumor suppressor, which induces p53-dependent senescence of HPV-positive HeLa cervical cancer cells. Oncogene 2009;28:762–72.
26. Nogueira V, Park Y, Chen CC, et al. Akt determines replicative senescence and oxidative or oncogenic premature senescence and sensitizes cells to oxidative apoptosis. Cancer Cell 2008;14:458–70.
27. Campaner S, Doni M, Hydbring P, et al. Cdk2 suppresses cellular senescence induced by the c-myc oncogene. Nat Cell Biol 12:54–9, sup pp 1–14.
28. Chandeck C, Mooi WJ. Oncogene-induced cellular senescence. Adv Anat Pathol 2009;17:42–8.
29. Caino MC, Meshki J, Kazanietz MG. Hallmarks for senescence in carcinogenesis: novel signaling players. Apoptosis 2009;14:392–408.
30. Courtois-Cox S, Jones SL, Cichowski K. Many roads lead to oncogene-induced senescence. Oncogene 2008;27:2801–9.
31. Kuilman T, Michaloglou C, Vredeveld LC, et al. Oncogene-induced senescence relayed by an interleukin-dependent inflammatory network. Cell 2008;133:1019–31.
32. Coppe JP, Patil CK, Rodier F, et al. Senescence-associated secretory phenotypes reveal cell-nonautonomous functions of oncogenic RAS and the p53 tumor suppressor. PLoS Biol 2008;6:2853–68.

Published OnlineFirst July 20, 2010; DOI: 10.1158/1541-7786.MCR-10-0174

33. Cichowski K, Hahn WC. Unexpected pieces to the senescence puzzle. Cell 2008;133:958–61.
34. Bartkova J, Rezaei N, Liontos M, et al. Oncogene-induced senescence is part of the tumorigenesis barrier imposed by DNA damage checkpoints. Nature 2006;444:633–7.
35. Bartek J, Bartkova J, Lukas J. DNA damage signalling guards against activated oncogenes and tumour progression. Oncogene 2007;26:7773–9.
36. Maclaine NJ, Hupp TR. The regulation of p53 by phosphorylation: a model for how distinct signals integrate into the p53 pathway. Aging (Albany NY) 2009;1:490–502.
37. Matsuoka S, Rotman G, Ogawa A, Shiloh Y, Tamai K, Elledge SJ. Ataxia telangiectasia-mutated phosphorylates Chk2 *in vivo* and *in vitro*. Proc Natl Acad Sci U S A 2000;97:10389–94.
38. Dimri GP. What has senescence got to do with cancer? Cancer Cell 2005;7:505–12.
39. Campisi J. Senescent cells, tumor suppression, and organismal aging: good citizens, bad neighbors. Cell 2005;120:513–22.
40. Wang Y, Blandino G, Givol D. Induced p21waf expression in H1299 cell line promotes cell senescence and protects against cytotoxic effect of radiation and doxorubicin. Oncogene 1999;18:2643–9.
41. Schmitt CA, Fridman JS, Yang M, et al. A senescence program controlled by p53 and p16INK4a contributes to the outcome of cancer therapy. Cell 2002;109:335–46.
42. Fang L, Igarashi M, Leung J, Sugrue MM, Lee SW, Aaronson SA. p21Waf1/Cip1/Sdi1 induces permanent growth arrest with markers of replicative senescence in human tumor cells lacking functional p53. Oncogene 1999;18:2789–97.
43. te Poele RH, Okorokov AL, Jardine L, Cummings J, Joel SP. DNA damage is able to induce senescence in tumor cells *in vitro* and *in vivo*. Cancer Res 2002;62:1876–83.
44. Kim KS, Kang KW, Seu YB, Baek SH, Kim JR. Interferon-γ induces cellular senescence through p53-dependent DNA damage signaling in human endothelial cells. Mech Ageing Dev 2009;130:179–88.
45. Banito A, Rashid ST, Acosta JC, et al. Senescence impairs successful reprogramming to pluripotent stem cells. Genes Dev 2009;23:2134–9.
46. DeNicola GM, Tuveson DA. RAS in cellular transformation and senescence. Eur J Cancer 2009;45 Suppl 1:211–6.
47. Rodier F, Coppe JP, Patil CK, et al. Persistent DNA damage signalling triggers senescence-associated inflammatory cytokine secretion. Nat Cell Biol 2009;11:973–9.
48. Hudson CD, Morris PJ, Latchman DS, Budhram-Mahadeo VS. Brn-3a transcription factor blocks p53-mediated activation of proapoptotic target genes Noxa and Bax *in vitro* and *in vivo* to determine cell fate. J Biol Chem 2005;280:11851–8.
49. Zemskova M, Sahakian E, Bashkirova S, Lilly M. The PIM1 kinase is a critical component of a survival pathway activated by docetaxel and promotes survival of docetaxel-treated prostate cancer cells. J Biol Chem 2008;283:20635–44.
50. Xu J. Preparation, culture, and immortalization of mouse embryonic fibroblasts. Curr Protoc Mol Biol 2005;Chapter 28:Unit 28.1.
51. Kueng W, Silber E, Eppenberger U. Quantification of cells cultured on 96-well plates. Anal Biochem 1989;182:16–9.
52. Majumder PK, Grisanzio C, O'Connell F, et al. A prostatic intraepithelial neoplasia-dependent p27 Kip1 checkpoint induces senescence and inhibits cell proliferation and cancer progression. Cancer Cell 2008;14:146–55.
53. Noda A, Ning Y, Venable SF, Pereira-Smith OM, Smith JR. Cloning of senescent cell-derived inhibitors of DNA synthesis using an expression screen. Exp Cell Res 1994;211:90–8.
54. Acosta JC, O'Loghlen A, Banito A, et al. Chemokine signaling via the CXCR2 receptor reinforces senescence. Cell 2008;133:1006–18.
55. Wajapeyee N, Serra RW, Zhu X, Mahalingam M, Green MR. Oncogenic BRAF induces senescence and apoptosis through pathways mediated by the secreted protein IGFBP7. Cell 2008;132:363–74.
56. Narita M, Nunez S, Heard E, et al. Rb-mediated heterochromatin formation and silencing of E2F target genes during cellular senescence. Cell 2003;113:703–16.
57. Mikkers H, Nawijn M, Allen J, et al. Mice deficient for all PIM kinases display reduced body size and impaired responses to hematopoietic growth factors. Mol Cell Biol 2004;24:6104–15.
58. Okamura S, Arakawa H, Tanaka T, et al. p53DINP1, a p53-inducible gene, regulates p53-dependent apoptosis. Mol Cell 2001;8:85–94.
59. Ellisen LW, Ramsayer KD, Johannessen CM, et al. REDD1, a developmentally regulated transcriptional target of p63 and p53, links p63 to regulation of reactive oxygen species. Mol Cell 2002;10:995–1005.
60. Lee CH, Chung JH. The hCds1 (Chk2)-FHA domain is essential for a chain of phosphorylation events on hCds1 that is induced by ionizing radiation. J Biol Chem 2001;276:30537–41.
61. Paull TT, Rogakou EP, Yamazaki V, Kirchgessner CU, Gellert M, Bonner WM. A critical role for histone H2AX in recruitment of repair factors to nuclear foci after DNA damage. Curr Biol 2000;10:886–95.
62. Tanaka T, Halicka HD, Huang X, Traganos F, Darzynkiewicz Z. Constitutive histone H2AX phosphorylation and ATM activation, the reporters of DNA damage by endogenous oxidants. Cell Cycle 2006;5:1940–5.
63. Roh M, Song C, Kim J, Abdulkadir SA. Chromosomal instability induced by Pim-1 is passage-dependent and associated with dysregulation of cyclin B1. J Biol Chem 2005;280:40568–77.
64. Jung YS, Qian Y, Chen X. Examination of the expanding pathways for the regulation of p21 expression and activity. Cell Signal 2010;7:1003–12.
65. Stout BA, Bates ME, Liu LY, Farrington NN, Bertics PJ. IL-5 and granulocyte-macrophage colony-stimulating factor activate STAT3 and STAT5 and promote Pim-1 and cyclin D3 protein expression in human eosinophils. J Immunol 2004;173:6409–17.
66. Hu YL, Passegue E, Fong S, Largman C, Lawrence HJ. Evidence that the Pim1 kinase gene is a direct target of HOXA9. Blood 2007;109:4732–8.
67. Eiring AM, Harb JG, Neviani P, et al. miR-328 functions as an RNA decoy to modulate hnRNP E2 regulation of mRNA translation in leukemic blasts. Cell 2010;140:652–65.
68. Shay KP, Wang Z, Xing PX, McKenzie IF, Magnuson NS. Pim-1 kinase stability is regulated by heat shock proteins and the ubiquitin-proteasome pathway. Mol Cancer Res 2005;3:170–81.
69. Ma J, Arnold HK, Lilly MB, Sears RC, Kraft AS. Negative regulation of Pim-1 protein kinase levels by the B56β subunit of PP2A. Oncogene 2007;26:5145–53.
70. He HC, Bi XC, Dai QS, et al. Detection of pim-1 mRNA in prostate cancer diagnosis. Chin Med J (Engl) 2007;120:1491–3.
71. Reddy JP, Peddibhotla S, Bu W, et al. Defining the ATM-mediated barrier to tumorigenesis in somatic mammary cells following ErbB2 activation. Proc Natl Acad Sci U S A 107:3728–33.
72. Crescenzi E, Palumbo G, Brady HJ. Bcl-2 activates a programme of premature senescence in human carcinoma cells. Biochem J 2003;375:263–74.
73. Goeman F, Thormeyer D, Abad M, et al. Growth inhibition by the tumor suppressor p33ING1 in immortalized and primary cells: involvement of two silencing domains and effect of Ras. Mol Cell Biol 2005;25:422–31.
74. Tombor B, Rundell K, Oltvai ZN. Bcl-2 promotes premature senescence induced by oncogenic Ras. Biochem Biophys Res Commun 2003;303:800–7.
75. Michaelson JS, Leder P. RNAi reveals anti-apoptotic and transcriptionally repressive activities of DAXX. J Cell Sci 2003;116:345–52.
76. Gostissa M, Morelli M, Mantovani F, et al. The transcriptional repressor hDaxx potentiates p53-dependent apoptosis. J Biol Chem 2004;279:48013–23.
77. Budram-Mahadeo V, Morris PJ, Latchman DS. The Brn-3a transcription factor inhibits the pro-apoptotic effect of p53 and enhances cell cycle arrest by differentially regulating the activity of the p53 target genes encoding Bax and p21(CIP1/Waf1). Oncogene 2002;21:6123–31.
78. Zhang Y, Wang Z, Magnuson NS. Pim-1 kinase-dependent phosphorylation of p21Cip1/WAF1 regulates its stability and cellular localization in H1299 cells. Mol Cancer Res 2007;5:909–22.
79. Biggs JR, Kudlow JE, Kraft AS. The role of the transcription factor Sp1 in regulating the expression of the WAF1/CIP1 gene in U937 leukemic cells. J Biol Chem 1996;271:901–6.

Published OnlineFirst July 20, 2010; DOI: 10.1158/1541-7786.MCR-10-0174

80. Mallette FA, Ferbeyre G. The DNA damage signaling pathway connects oncogenic stress to cellular senescence. Cell Cycle 2007;6:1831–6.

81. Catalano A, Rodilossi S, Caprari P, Coppola V, Procopio A. 5-Lipoxygenase regulates senescence-like growth arrest by promoting ROS-dependent p53 activation. EMBO J 2005;24:170–9.

82. Chen Q, Fischer A, Reagan JD, Yan LJ, Ames BN. Oxidative DNA damage and senescence of human diploid fibroblast cells. Proc Natl Acad Sci U S A 1995;92:4337–41.

83. Di Micco R, Fumagalli M, Cicalese A, et al. Oncogene-induced senescence is a DNA damage response triggered by DNA hyper-replication. Nature 2006;444:638–42.

84. Halazonetis TD, Gorgoulis VG, Bartek J. An oncogene-induced DNA damage model for cancer development. Science 2008;319:1352–5.

85. Zhang Y, Parsanejad M, Huang E, et al. Pim-1 kinase as activator of the cell cycle pathway in neuronal death induced by DNA damage. J Neurochem 112:497–510.

86. Roh M, Franco OE, Hayward SW, van der Meer R, Abdulkadir SA. A role for polyploidy in the tumorigenicity of Pim-1-expressing human prostate and mammary epithelial cells. PLoS One 2008;3:e2572.

87. Roh M, Gary B, Song C, et al. Overexpression of the oncogenic kinase Pim-1 leads to genomic instability. Cancer Res 2003;63:8079–84.

88. Bhattacharya N, Wang Z, Davitt C, McKenzie IF, Xing PX, Magnuson NS. Pim-1 associates with protein complexes necessary for mitosis. Chromosoma 2002;111:80–95.

89. van Bokhoven A, Varella-Garcia M, Korch C, et al. Molecular characterization of human prostate carcinoma cell lines. Prostate 2003;57:205–25.

90. Morwick T. Pim kinase inhibitors: a survey of the patent literature. Expert Opin Ther Pat 20:193–212.

Published OnlineFirst July 20, 2010; DOI: 10.1158/1541-7786.MCR-10-0174

Molecular Cancer Research

p53-Dependent Induction of Prostate Cancer Cell Senescence by the PIM1 Protein Kinase

Marina Zemskova, Michael B. Lilly, Ying-Wei Lin, et al.

Mol Cancer Res 2010;8:1126-1141. Published OnlineFirst July 20, 2010.